Review

Michał Silarski*, Katarzyna Dziedzic-Kocurek and Monika Szczepanek

Combined BNCT and PET for theranostics

https://doi.org/10.1515/bams-2021-0140
Received September 12, 2021; accepted November 17, 2021;
published online November 30, 2021

Abstract: This short review summarizes the issue of boron distribution monitoring in boron neutron capture therapy (BNCT), which remains a serious drawback of this powerful oncological treatment. Here we present the monitoring methods that are presently used with particular emphasis on the positron emission tomography (PET) which has the highest potential to be used for the real-time monitoring of boron biodistribution. We discuss the possibility of using present PET scanners to determine the boron uptake *in vivo* before the BNCT treatment with the use of *p*-boronphenylalanine (BPA) labeled with ^{18}F isotope. Several examples of preclinical studies and clinical trials performed with the use of [^{18}F]FBPA are shown. We also discuss shortly the perspectives of using other radiotracers and boron carriers which may significantly improve the boron imaging with the use of the state-of-the-art Total-Body PET scanners providing a theranostic approach in the BNCT.

Keywords: BNCT therapy; dose distribution monitoring; PET tomography.

Introduction

The boron neutron capture therapy (BNCT) is a cancer treatment exploiting properties of the thermal neutron capture reactions proceeding with high probability on ^{10}B isotope. The BNCT treatment is done in two steps. First, a special carrier containing ^{10}B isotope is administered to a patient. Its role is to deliver as many boron atoms as possible to the tumor cells, preferably to the nucleus. The second step of the treatment is the irradiation with neutrons which begins after the boron concentration in the tumor reaches its maximum. The therapeutic beam contains epithermal neutrons with energies in the range of about 0.5 eV–40 keV [1] which lose their energy while passing through the patient's body. The energy loss originates from the neutron scattering on atoms composing human body. As a result, they thermalize while reaching the tumor where they can be captured by ^{10}B isotope in the following reaction:

$$n + {}^{10}\mathrm{B} \rightarrow \alpha + {}^{7}\mathrm{Li}^{*} \rightarrow \alpha + {}^{7}\mathrm{Li} + \gamma\,(478\ \mathrm{keV}),$$

where the α particle and lithium nucleus acquire energy equal in total to about 2.3 MeV.[1] In fact, in about 6.1% of neutron captures on ^{10}B proceeds with lithium nucleus in a ground state, for which the total energy of the two ions amounts to 2.79 MeV [2].

The main advantage of BNCT is the ability of selective destruction of cancer cells and its high biological effectiveness. The path length of the charged particles originating from the neutron capture on ^{10}B are of the order of a single cell size (about 10 μm and 5 μm for the α particle and Li nucleus, respectively [2]). Thus, due to the high linear energy transfer (LET) of the above mentioned reaction products, the BNCT treatment allows to kill the tumor cells with no significant harm to the healthy tissues [3]. This is possible due to the value of neutron capture cross-section on ^{10}B, equal to σ_c = 3,835 b [2], which is much higher than the cross-sections of any interaction with carbon, hydrogen, or nitrogen being of the order of 4–20 b [2]. The BNCT potential to selectively increase the radiation dose in the tumor cells determined its clinical use concentrated on the head and neck tumors and deep-seated and disseminated brain tumors which are hard or impossible to remove surgically. BNCT has also been applied when the side effects of the other oncological treatments are not acceptable [2], and to treat malignant melanoma [1].

It is worth to mention that there are other elements with even higher interaction probabilities which could be used as targets for neutron capture therapy. Among them, gadolinium (Gd) was considered as an alternative for boron, but so far there is no carrier which can effectively deliver Gd to the tumor cells nuclei. Moreover, the neutron

*Corresponding author: Michal Silarski, Faculty of Physics, Astronomy and Applied Computer Science, Jagiellonian University, 30-348 Cracow, Poland; and Total-Body Jagiellonian-PET Laboratory, Jagiellonian University, Cracow, Poland,
E-mail: michal.silarski@uj.edu.pl
Katarzyna Dziedzic-Kocurek, Faculty of Physics, Astronomy and Applied Computer Science, Jagiellonian University, Cracow, Poland
Monika Szczepanek, Faculty of Physics, Astronomy and Applied Computer Science, Jagiellonian University, Cracow, Poland; and Total-Body Jagiellonian-PET Laboratory, Jagiellonian University, Cracow, Poland

capture (mostly on the ^{157}Gd) results, in this case, in the emission of γ quanta with energies ranging from 0.08 to 7.8 MeV which do not provide short-range energy deposition as in the case of ^{10}B [4].

One of the major issues in BNCT is delivering boron to the tumor cells with subsequent lowest possible concentration in the healthy tissues. To meet this clinical need, two boron carriers have been developed and used: BSH (sodium borocaptate, $Na_2B_{12}H_{11}SH$) [5, 6] and BPA (p-boronphenylalanine, $C_9H_{12}BNO_4$). So far only BPA was approved as a drug in Japan [7]. They reveal, however, several disadvantages, like non-uniform uptake of boron in the cancer cells. Moreover, their application is limited to only a few types of cancer [8].

Until recently another major obstacle in the introduction of BNCT into hospitals was the neutron sources limited to the nuclear reactors. This situation has changed recently due to the rapid development of accelerator-based neutron sources which nowadays are able to provide the appropriate beam intensities (~10^9·1/[cm^2 s]) [9, 10]. Beams provided by these sources contain, apart from the therapeutic epithermal neutrons, γ quanta, as well as fast and thermal neutrons. These additional components should be minimized in terms of neutron flux and delivered dose rate since they are the main cause of side effects in the therapy (e.g. in the case of deep-seated brain tumors treatment, the thermal neutrons can damage the scalp of a patient). Moreover, the mixed fields of radiation in BNCT complicate the patient's dosimetry, treatment planning, and therapy monitoring. The latter issue concerns mainly ^{10}B distribution in the patient's body that may be solved using the positron emission tomography (PET).

Boron distribution monitoring in BNCT

There are several methods used for accurate measurement of the ^{10}B concentration in tissues and fluids, such as blood and urine, and for determination of its microscopic spatial distribution at the cellular or subcellular level. Ideally, these methods should be noninvasive, allowing *in vivo* measurements in the patient, and fast so that they enable clinical decisions based on their results [11].

For the *in vitro* boron distribution determination, several methods were proven to be useful. The inductively coupled plasma mass spectrometry (ICP-MS) joins an inductively coupled plasma as a method of ionization with mass spectrometry for separating and detecting the ions. ICP-MS can separate the two boron isotopes (namely ^{10}B and ^{11}B) and quantify boron concentration at ppb levels in serum, plasma, urine, saline, water, and tissues [11]. High-resolution alpha-track autoradiography (HRAR) may be used for small tissue samples. It takes advantage of the registration of tracks generated by alpha particles and Li ions in nuclear films. This method requires frozen tissue sections with the thickness of the order of micrometers mounted on top of sub-micrometer thick *Ixan* and *Lexan* films which are next irradiated with thermal neutrons [11]. After the irradiation, the tissue is histologically stained and the use of microtomography allows to map the ^{10}B distribution in the tissue by correlating the distribution of tracks in the films with the anatomical features of the stained tissue. A similar approach is used in Neutron Capture Radiography. Here a sample should be a few millimeters thick with a minimal surface of 0.5 cm^2 and it is frozen in liquid nitrogen and divided into three parts. One of them is analyzed histopathologically and the other two are fixed on nuclear detection films and irradiated with thermal neutrons. The charged ions resulting in the neuron capture on the ^{10}B isotope are able to exit the sample and their tracks are registered in the films. The information gathered for all the samples is merged at the end of a procedure giving a two-dimensional distribution of ^{10}B in the sample with a resolution of about 100 μm and sensitivity of the order of ppm [11]. There are several other methods, like laser post-ionization secondary neutral mass spectrometry (LPI SNMS), electron energy loss spectroscopy (EELS), or ion trap mass spectrometry (ITMS) which were used to determine the boron uptake at the cellular level, but they all need the support of biopsy.

Among the methods providing the *in vitro* boron concentration measurements, the magnetic resonance imaging (MRI) and prompt gamma radiation analysis (PGRA) have a potential to be used *in vivo* in the near future. MRI is based on the interaction of magnetic moments of nuclei with external magnetic fields. The strong and constant magnetic field spins of the nuclei align along its axis which results in the generation of nonzero magnetization $\vec{M}$ of the tissue. An additional oscillating magnetic field changes the direction of $\vec{M}$ which is precessing around the $\vec{B_0}$ with a characteristic frequency. The additional gradient fields allow for excitation of different voxels of the body and perform imaging. There are two relaxation times characterizing the longitudinal (T_1) and transverse components (T_2) of the magnetization. These times are essential for the sensitivity and spatial resolution of the MRI imaging which depends on the ^{10}B compound administered in the patient's body. In general, this method is able to detect and distinguish ^{10}B and ^{11}B isotopes (a natural abundance of these boron isotopes is equal to 19% and 81%, respectively) and

their direct detection is possible in the case of BSH, while for BPA, more advantageous may be a measurement of hydrogen concentration [12, 13]. However, due to the low sensitivity in the case of *in vivo* imaging with the presently used MRI scanners, the direct quantification of boron is done so far only *in vitro* [11]. For BPA, the performance of MRI detection may be improved by introducing other elements which increase the ferromagnetic properties of this boron carrier. ^{19}F-BPA was successfully applied for *in vivo* spatial distribution mapping of boron uptake in a rat brain, showing a big potential to use MRI in BNCT treatment planning [14]. The other possible direction towards monitoring the boron distribution during the BNCT treatment is to apply a carrier containing gadolinium, preferably ^{157}Gd isotope which would additionally lead to dual B-GdNCT. Such conjugation was tested using $GdBO_3$–Fe_3O_4 nanocomposites [15] and low-density lipoproteins (LDL) [16]. However, the typical clinical MRI scanners are not yet suitable for boron imaging [13] and they are used in clinics only to monitor the tumor volume before and after BNCT and to quantify the carrier uptake *in vitro*, e.g. in blood samples [17].

The other method revealing the potential to provide information about the administered dose in real-time during the treatment is the prompt gamma radiation analysis (PGRA). It is based on a registration of γ quanta emitted as a result of the neutron beam interactions with the tumor and surrounding tissues. The basic neutron capture reaction on ^{10}B isotope results, in most of the cases, in the emission of the 478 keV γ quantum which enables determination of the spatial distribution of the administered boron carrier. The reconstruction of the γ quanta emission points requires the application of dedicated detector systems based on the single photon emission computed tomography (SPECT) or Compton Camera solutions. There are, however, several technical issues to be addressed before these methods will be used for the *in vivo* measurements. So far, the commonly used SPECT devices are not able to measure the 478 keV line due to the γ rays background induced by the BNCT neutron beam. The limiting factors include the total efficiency of registration of the above-mentioned γ rays and the energy resolution of the used detectors. They should provide separation of the line of interest from the 511 keV γ rays. This radiation is produced mainly as a byproduct of the pair creation of the 2.2 MeV hydrogen γ rays in the patient's body. The efficiency affects the statistical precision of the measurement which is additionally limited by the neutron capture rate [18]. There were several attempts to design a PGRA-SPECT imaging system based inter alia on the CdZnTe semiconductors [19] or $LaBr_3$(Ce) and $LaCl_3$(Ce) scintillators [20], but there are no such devices working in clinics. An interesting idea is the combination of PGRA-SPECT with PET imaging which may give additional information on the thermal neutron flux distribution. It may be obtained also in the tissues which do not contain boron by registration of the 2.2 MeV γ quanta from the neutron capture on hydrogen. As we present in the next section, PET appears to be the only *in vivo* imaging modality for quantification of the ^{10}B distribution prior to the BNCT treatment and it has the potential to be useful also for the real-time monitoring.

PET application in BNCT

The positron emission tomography is a powerful tool in biomedical research and clinical practice. It relays, as in the case of BNCT, on pharmaceuticals labeled with a short-lived positron-emitting element which are selectively accumulated in tumors. There are several β^+ emitters which can be used to trace the metabolism of the used pharmaceutical (ligand) which differ in the mean lifetime and maximum positron energy which limit the intrinsic spatial resolution of the method. For example, the most popular amino acid tracer used in PET imaging of brain tumors is ^{11}C-methionine [21].

The other commonly used radionuclide is ^{18}F with a glucose molecule where the fluorine substitutes one of the OH groups forming fluorodeoxyglucose (FDG) [22, 23]. The first successful trial to introduce the radiotracer to the ^{10}B carrier was made in 1991 by synthesis of the 4-^{10}B-Borono-2-^{18}F-fluoro-L-phenylalanine ([^{18}F]FBPA, see Figure 1) for *in vivo* monitoring of the BPA biodistribution [17, 24, 25]. [^{18}F]FBPA was tested on animal models and recently has been also clinically applied in Japan. Examples of these studies are given in the next subsections.

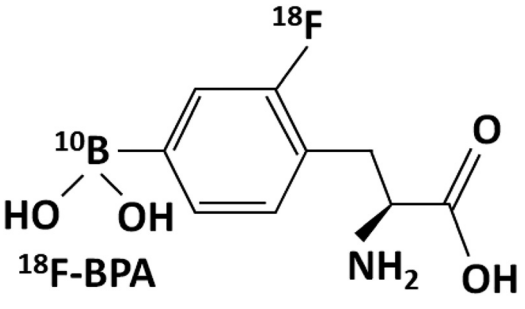

Figure 1: Chemical structure of the [^{18}F]FBPA used in the PET imaging for BNCT.

Preclinical studies of [^{18}F]FBPA biodistribution

Most of the preclinical studies were done on animals (e.g. mice [26, 27], hamsters [28], rats [29]) and some of them on cell lines (e.g. human glioblastoma T98G [30]). It was shown that the melanogenesis in tumors is enhancing the uptake of [^{18}F]FBPA and the L-form of this compound was preferentially accumulated in melanoma compared with the D-isomer [28]. Studies on mice showed the highest accumulation of [^{18}F]FBPA in the pancreas, liver, spleen, small intestine and testis at 5–10 min after injection, while brain uptake was constant for 2 h and was the lowest. High tumor-to-tissue uptake ratios were observed for all organs, except for a kidney, at 2 h post-injection while about half of the injected tracer was recovered in the urines [24, 30]. Human glioblastoma T98G cells were used to examine the cellular distribution of [^{18}F]FBPA by labeling with a stable fluoride isotope ^{19}F for the MRI imaging. It was shown that this compound is accumulated in the nucleus and cytoplasm. These results also confirmed that there is no decomposition of the [^{19}F]FBPA in tumor cells [25].

Clinical trials using [^{18}F]FBPA

The first BNCT clinical trials with [^{18}F]FBPA as ^{10}B carrier were done in 2006 with the PET scan performed before the treatment which indicated the tumor/normal tissue boron concentration ratio equal to 2.9 [31].

The [^{18}F]FBPA was used to treat metastatic malignant melanoma for which the ^{10}B concentration was found to be four times higher than for the normal tissue 40 min after injection [32]. The other studies were performed for gliomas, metastatic brain melanoma, sinonasal undifferentiated carcinoma, schwannoma, meningioma, and oral cancer [17, 32].

Despite the rather positive outcomes of the clinical trials, the [^{18}F]FBPA is not yet a complete candidate for the theranostic solution in BNCT [17]. Pharmacokinetics of [^{18}F]-FBPA is very similar to that of BPA, although there are slight discrepancies between these two compounds [25]. Moreover, the concentration of [^{18}F]FBPA needed for the BNCT treatment is much higher than the one for an accurate PET scan [17]. This may significantly decrease the signal to noise ratio for the PET scanner if the tomography would be performed during the irradiation with neutron beam. Thus, the use of [^{18}F]FBPA is limited to clinical trials only until it will be accepted as a drug [17].

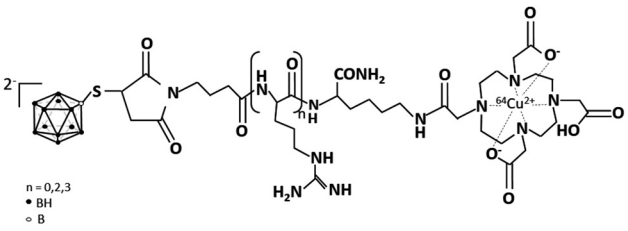

Figure 2: Chemical structures of BSH peptide fused with 1,4,7,10-tetraazacyclododecane-1,4,7,10-tetraacetic acid (DOTA). Figure adapted from ref. [33].

Apart from ^{18}F, there are other possible radiotracers which may be used for monitoring in BNCT. Promising results for brain tumor uptake were observed for a derivative of the BSH fused with arginine peptide and labeled with the ^{64}Cu isotope [17, 33], as shown in Figure 2. The pharmacokinetics of this compound was tested on a mouse model, and it showed that the BSH-3R pharmacokinetics correlates well with the real ^{10}B concentration. The advantages of ^{64}Cu over ^{18}F are its higher lifetime and easier linking to the boron agent via DOTA antibody [33]. The third-generation boron agents which have been developed in recent years may be labeled with isotopes of I, In, Ga, or Lu. For example, the gold nanoparticles were successfully labeled with ^{124}I and tested on a mouse model of human fibrosarcoma, but the boron uptake was too low for the effective BNCT treatment. The other nanoparticles which can be labeled for the PET scan are boron nitride nanoparticles coupled to ^{64}Cu isotope, but they again appeared to be not effective enough [17].

Total-body PET development: a step towards theranostics

The development of a new generation boron carriers and the possible theranostic approach in BNCT due to their labeling with β^+ radionuclide or an element enabling the MRI imaging (e.g. Gd or ^{19}F) is particularly interesting in view of the new Total-Body PET technology [34]. Extension of the field of view (FOV) from the standard 20 cm up to 200 cm increases the sensitivity a dozen times and enables monitoring of the whole patient's body at the same time [35]. The first Total-Body PET tomograph, uEXPLORER, was introduced in the USA in 2018 [36, 37]. It is built out of $2.76 \times 2.76 \times 19.1$ mm^3 LYSO pixels read out by silicon photomultipliers. The axial length of this detection system amounts to about 194 cm and is characterized by 3 mm spatial resolution which implied quite a large number of detector crystals to be used [35]. The first clinical studies

revealed that total-body pharmacokinetic studies can be done within a time slot of 1 s with a significantly improved signal-to-noise ratio. This, in turn, allows the decrease in activity of the FDG which needs to be administered to the patient and shorten the examination time [37]. uEXPLORER was combined with an 80 detectors row CT. The major disadvantage of this PET solution impeding its wide use in the medical centers is the high cost, driven mainly by the prices of the detection crystals [34, 35]. One of the possible ways to reduce the cost of the Total-Body PET scanner is using plastic scintillators, which are much cheaper and much easier to produce than the inorganic crystal detectors [38–40]. This, however, requires changing the detection paradigm, since plastic scintillators do not provide a good measurement of the annihilation γ quanta. In turn, they are characterized by much better time resolution, compared to that of crystals, and high light attenuation length which allows the construction of long detection modules [34, 41–44]. The only tomography system based on the long plastic scintillator detectors is the Jagiellonian-PET (J-PET) developed at the Jagiellonian University, Cracow, Poland. J-PET may offer the extension of the FOV up to even 250 cm with high and uniform sensitivity over the whole human body [34, 45–47]. The low weight and high modularity of J-PET enables reconfiguration of the tomographic volume and it is an advantage in view of the BNCT monitoring. In Figure 3, we present a photograph of the plastic digital J-PET prototype consisting of 24 modules arranged axially with 50 cm FOV. Each module contains 13 optically separated plastic scintillator strips read-out on both ends with a matrix of four silicon photomultipliers. The position and time of the interaction of annihilation γ quanta are determined by measurement of the times when the scintillation light signals arrived at the edges of the strips [34, 39, 43].

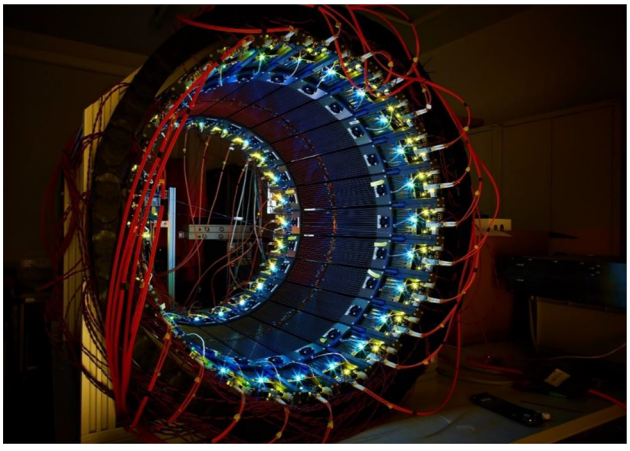

Figure 3: A photograph showing the 50 cm FOV modular J-PET prototype. Courtesy of the J-PET collaboration.

Dedicated electronics was developed for registration of the SiMPs signals with the time accuracy of approximately 20 ps [48]. The novelty is the triggerless and reconfigurable data acquisition system [49]. The modularity and possibility of easily changing the geometry of the J-PET scanner together with the triggerless acquisition mode open new possibilities in the simultaneous imaging of the human body with different techniques. In principle, J-PET could be combined with MRI or CT scanners [50, 51], which could not only improve the quality of the treatment planning, but also provide simultaneous positronium imaging [52–56] and monitoring the metabolic activity during the BNCT treatment [34, 52, 53]. The other advantage of the J-PET technology is the ability of multiphoton imaging which improves the spatial resolution and opens the possibility of simultaneous imaging with different tracers [34]. This solution might be applied as a theranostic tool in BNCT, since focusing on the multi-coincidence events may significantly reduce the noise level for the PET imaging during the therapy.

Here one can take advantage of radioisotopes for which the β^+ decay results in an excited nucleus which subsequently emits a prompt γ quantum (so-called $\beta^+\gamma$ emitters [34]). Among many $\beta^+\gamma$ emitters [57] used for this diagnostic mode, candidates such as ^{124}I, ^{110m}In, ^{66}Ga, or ^{60}Cu may be of interest in view of BNCT monitoring and they have been already considered for labeling the new boron carriers.

Conclusions

BNCT is a two-step treatment modality which relies on precise delivery of boron ^{10}B isotope to a tumor with simultaneous low accumulation in the blood and healthy tissues. With the development of accelerator-based sources, the main open issues of BNCT are the boron carriers suitable for effective boron delivery to cancer, and the *in vivo* determination of the biodistribution of ^{10}B isotope. Such information is important mainly in the treatment planning and evaluation of BNCT effects. Among the available methods of boron monitoring, PET seems to be the most promising since this method may provide not only imaging of ^{10}B spatial distribution before the treatment, but also may enable real-time monitoring. The only compound used so far in clinical studies is the [^{18}F]FBPA, one of the two commonly used carriers labeled with the ^{18}F isotope. These studies were promising, especially in melanoma, glioblastoma, and head and neck cancer treatment. However, there are several obstacles preventing the successful application of PET scanners for real-time monitoring. One

of them is the much higher concentration of the labeled boron carrier which is needed for the therapy than for the PET scan itself. The neutron and γ ray fields in which the PET scanner must work during the therapy are also important. The other crucial limitation is also the small field of view of the commonly used PET scanners. The solution may be the total-body PET scanner which has the potential to image the whole body of a patient with better sensitivity and resolution [34, 37, 54]. Among all the total-body PET solutions, the J-PET tomograph, based on cost-effective plastic scintillators, has a high potential towards successful real-time boron monitoring. Having the possibility of its combination with the MRI or CT modalities it would be, together with the new boron carriers, a breakthrough towards theranostic in BNCT.

Research funding: This work has been supported by Grants U1U/P05/NW/03.23 and U1U/P05/NO/03.47 from the SciMat Priority Research Area under the Strategic Programme Excellence Initiative at the Jagiellonian University. We acknowledge the support from the Polish National Centre for Research and Development through Grant No. LIDER/17/0046/L-7/15/NCBR/2016 and from the Priority Research Area DigiWorld under the program Excellence Initiative-Research University at the Jagiellonian University in Kraków. The founding organizations played no role in the study design; in the collection, analysis, and interpretation of data; in the writing of the report; or in the decision to submit the report for publication.

Author contributions: All authors have accepted responsibility for the entire content of this manuscript and approved its submission.

Competing interests: Authors state no conflict of interest.

Informed consent: Not applicable.

Ethical approval: Not applicable.

References

1. Japanese Society of Neutron Capture Therapy. What is BNCT? [Online]. Available from: http://www.jsnct.jp/e/about_nct/gen.html [Accessed 24 Aug 2021].
2. Sauerwein WAG. Principles and roots of neutron capture therapy. In: Sauerwein WAG, Wittig A, Moss R, Nakagawa Y, editors. Neutron capture therapy: principles and applications. Berlin Heidelberg: Springer-Verlag; 2012.
3. Nedunchezhian K, Aswath N, Thiruppathy M, Thirugnanamurthy S. Boron neutron capture therapy-A literature review. J Clin Diagn Res 2016;10:ZE01–4.
4. Enger SA, Giusti V, Fortin M-A, Lundqvist H, Rosenschöld PM. Dosimetry for gadolinium neutron capture therapy (GdNCT). Radiat Meas 2013;59:233–40.
5. Gibson CR, Staubus AE, Barth RE, Yang W, Ferkefich AK, Moeschberger MM. Pharmacokinetics of sodium borocaptate: a critical assessment of dosing paradigms for boron neutron capture therapy. J Neuro Oncol 2003;62:157–69.
6. Michiue H, Sakurai Y, Kondo N, Kitamatsu M, Bin F, Nakajima K, et al. The acceleration of boron neutron capture therapy using multi-linked mercaptoundecahydrododecaborate (BSH) fused cell-penetrating peptide. Biomaterials 2014;35:3396–405.
7. Stella Pharma Corporation. News release: STELLA PHARMA will launch Steboronine®, the World's first BNCT drug, on May 20; 2020. Available from: https://stella-pharma.co.jp/cp-bin/wordpress5/wp-content/uploads/2020/05/Steboronine-launched_ENG.pdf [Accessed 25 Aug 2021].
8. Nakamura H, Kirihata M. Boron compounds: new candidates for boron carriers in BNCT, principles and roots of neutron capture therapy. In: Sauerwein WAG, Wittig A, Moss R, Nakagawa Y, editors. Neutron capture therapy: principles and applications. Berlin Heidelberg: Springer-Verlag Berlin Heidelberg; 2012.
9. Taskaev S, Berendeev E, Bikchurina M, Bykov T, Kasatov D, Kolesnikov I, et al. Neutron source based on vacuum insulated tandem accelerator and lithium target. Biology 2021;10:350.
10. Kreiner AJ. Accelerator-based BNCT. In: Sauerwein WAG, Wittig A, Moss R, Nakagawa Y, editors. Neutron capture therapy: principles and applications. Berlin Heidelberg: Springer-Verlag; 2012.
11. Wittig A, Sauerwein WAG. Boron analysis and boron imaging in BNCT. In: Sauerwein WAG, Wittig A, Moss R, Nakagawa Y, editors. Neutron capture therapy: principles and applications. Berlin Heidelberg: Springer-Verlag; 2012.
12. Bendel P, Sauerwein W. Optimal detection of the neutron capture therapy agent borocaptate sodium (BSH): a comparison between ^{1}H and ^{10}B NMR. Med Phys 2001;28:178.
13. Timonen M, Kankaanranta L, Lundbom N, Collan J, Kangasmaki A, Kortesniemi M, et al. ^{1}H MRS studies in the Finnish boron neutron capture therapy project: detection of ^{10}B-carrier, L-*p*-boronophenylalanine-fructose. Eur J Radiol 2005;56:154–9.
14. Porcari P, Capuani S, D'Amore E, Lecce M, La Bella A, Fasano F, et al. In vivo ^{19}F MR imaging and spectroscopy for the BNCT optimization. Appl Radiat Isot 2009;67:S365–8.
15. Icten O, Ali Kose D, Matissek SJ, Misurelli JA, Elsawa SF, Hosmane NS, et al. Gadolinium borate and iron oxide bioconjugates: nanocomposites of next generation with multifunctional applications. Mater Sci Eng C 2018;92:317–28.
16. Alberti D, Protti N, Toppino A, Deagostino A, Lanzardo S, Bortolussi S, et al. A theranostic approach based on the use of a dual boron/Gd agent to improve the efficacy of Boron Neutron Capture Therapy in the lung cancer treatment. Nanomed Nanotechnol Biol Med 2015;11:741–50.
17. Sauerwein WAG, Sancey L, Hey-Hawkins E, Kellert M, Panza L, Imperio D, et al. Theranostics in boron neutron capture therapy. Life 2021;11:330.
18. Valda A, Minsky DM, Kreiner AJ, Burlon AA, Somacal H. Development of a tomographic system for online dose measurements in BNCT (boron neutron capture therapy). Braz J Phys 2005;35:785.
19. Manabe M, Nakamura S, Murata I. Study on measuring device arrangement of array-type CdTe detector for BNCT-SPECT. Rep Radiother Oncol 2016;21:102–7.

20. Gong C, Tang X, Fatemi S, Yu H, Shao W, Shu D, et al. A Monte Carlo study of SPECT in boron neutron capture therapy for a heterogeneous human phantom. Int J Radiat Res 2018;16:33–43.
21. Glaudemans AW, Enting RH, Heesters MA, Dierckx RA, van Rheenen RW, Walenkamp AM, et al. Value of ^{11}C-methionine PET in imaging brain tumours and metastases. Eur J Nucl Med Mol Imag 2013;40:615–35.
22. Sharma R, D'Souza M, Jaimini A, Hazari PP, Saw S, Pandey S, et al. A comparison study of (11)C-methionine and (18) F-fluorodeoxyglucose positron emission tomography-computed tomography scans in evaluation of patients with recurrent brain tumors. Indian J Nucl Med 2016;31:93–102.
23. Alavi A, Hess S, Werner TJ, Høilund-Carlsen PF. An update on the unparalleled impact of FDG-PET imaging on the day-to-day practice of medicine with emphasis on management of infectious/inflammatory disorders. Eur J Nucl Med Mol Imag 2020;47:18–27.
24. Ishiwata K, Ido T, Mejia AA, Ichihashi M, Mishima Y. Synthesis and radiation dosimetry of 4-borono-2-[^{18}F]fluoro-D,Lphenylalanine: a target compound for PET and boron neutron capture therapy. Int J Radiat Appl Instrum A 1991;42:325–8.
25. Ishiwata K. 4-Borono-2-^{18}F-fluoro-l-phenylalanine PET for boron neutron capture therapy-oriented diagnosis: overview of a quarter century of research. Ann Nucl Med 2019;33:223–36.
26. Ishiwata K, Ido T, Kawamura M, Kubota K, Ichihashi M, Mishima Y. 4-Borono-2-[^{18}F]fluoro-d,l-phenylalanine as a target compound for boron neutron capture therapy: tumor imaging potential with positron emission tomography. Nucl Med Biol 1991;18:745–51.
27. Coderre JA, Glass JD, Fairchild RG, Roy U, Cohen S, Fand I. Selective targeting of boronophenylalanine to melanoma in BALB/c mice for neutron capture therapy. Cancer Res 1987;47: 6377–83.
28. Ishiwata K, Ido T, Honda C, Kawamura M, Ichihashi M, Mishima Y. 4-Borono-2-[^{18}F]fluoro-d,l-phenylalanine: a possible tracer for melanoma diagnosis with PET. Nucl Med Biol 1992;19:311–8.
29. Wang HE, Liao AH, Deng WP, Chang PF, Chen JC, Chen FD, et al. Evaluation of 4-borono-2-^{18}F-fluoro-l-phenylalaninefructose as a probe for boron neutron capture therapy in a glioma bearing rat model. J Nucl Med 2004;45:302–8.
30. Evangelista L, Jori G, Martini D, Sotti G. Boron neutron capture therapy and ^{18}F-labelled borophenylalanine positron emission tomography: a critical and clinical overview of the literature. Appl Radiat Isot 2013;74:9–101.
31. Aihara T, Hiratsuka J, Morita N, Uno M, Sakurai Y, Maruhashi A, et al. First clinical case of boron neutron capture therapy for head and neck malignancies using ^{18}F-BPA PET. Case Rep 2006;28: 850–5.
32. Kabalka GW, Nichols TL, Smith GT, Miller LF, Khan MK, Busse PM. The use of positron emission tomography to develop boron neutron capture therapy treatment plans for metastatic malignant melanoma. J Neurooncol 2003;62:187–95.
33. Iguchi Y, Michiue H, Kitamatsu M, Hayashi Y, Takenaka F, Nishiki T, et al. Tumor-specific delivery of BSH-3R for boron neutron capture therapy and positron emission tomography imaging in a mouse brain tumor model. Biomaterials 2015;56:10–7.
34. Moskal P, Stępień EŁ. Prospects and clinical perspectives of total-body PET imaging using plastic scintillators. Pet Clin 2020;15: 439–45.
35. Vandenberghe S, Moskal P, Karp JS. State of the art in total body PET. EJNMMI Phys 2020;7:35.
36. Cherry S, Karp J, Moses W, Qi J, Bec J, Berg E, et al. EXPLORER: an ultra-sensitive total-body PET scanner for biomedical research. In: Proceedings of IEEE nuclear science symposium and medical imaging conference; 2013:M03–01 pp.
37. Badawi RD, Shi H, Hu P, Chen S, Xu T, Price PM, et al. First human imaging studies with the EXPLORER total-body PET scanner. J Nucl Med 2019;60:299–303.
38. Moskal P, Salabura P, Silarski M, Smyrski J, Zdebik J, Zieliński M. Novel detector systems for the positron emission tomography. Bio-Algorithms Med-Syst. 2011;7:73–8.
39. Moskal P, Niedźwiecki Sz, Bednarski T, Czerwiński E, Kapłon Ł, Kubicz E, et al. Test of a single module of the J-PET scanner based on plastic scintillators. Nucl Instrum Methods Phys Res A 2014; 764:317–21.
40. Moskal P, Zoń N, Bednarski T, Białas P, Czerwiński E, Gajos A, et al. A novel method for the line-of-response and time-of-flight reconstruction in TOF-PET detectors based on a library of synchronized model signals. Nucl Instrum Methods A 2015;775: 54–62.
41. Kapłon Ł. Technical attenuation length Measurement of plastic scintillator strips for the total-body J-PET scanner. IEEE Trans Nucl Sci 2020;67:2286–9.
42. Kapłon Ł, Moskal G. Blue-emitting polystyrene scintillators for plastic scintillation dosimetry. Bio-Algorithms Med-Syst 2021;17: 191–7.
43. Moskal P, Rundel O, Alfs D, Bednarski T, Białas P, Czerwiński E, et al. Time resolution of the plastic scintillator strips with matrix photomultiplier readout for J-PET tomograph. Phys Med Biol 2016;61:2025.
44. Wieczorek A, Dulski K, Niedźwiecki Sz, Alfs D, Białas P, Curceanu C, et al. Novel scintillating material 2-(4-styrylphenyl) benzoxazole for the fully digital and MRI compatible J-PET tomograph based on plastic scintillators. PLoS ONE 2017;12: e0186728.
45. Moskal P, Kowalski P, Shopa RY, Raczyński L, Baran J, Chug N, et al. Simulating NEMA characteristics of the modular total-body J-PET scanner—an economic total-body PET from plastic scintillators. Phys Med Biol 2021;66:175015.
46. Raczyński L, Wiślicki W, Klimaszewski K, Krzemień W, Kopka P, Kowalski P, et al. 3D TOF-PET image reconstruction using total variation regularization. Phys Med 2020;80: 230–42.
47. Shopa RY, Klimaszewski K, Kopka P, Kowalski P, Krzemień W, Raczyński L, et al. Optimisation of the event-based TOF filtered back-projection for online imaging in total-body. J-PET Med Image Anal 2021;73:102199.
48. Pałka M, Strzempek P, Korcyl G, Bednarski T, Niedźwiecki Sz, Białas P, et al. Multichannel FPGA based MVT system for high precision time (20 ps RMS) and charge measurement. J Instrum 2017;12:P08001.
49. Korcyl G, Białas P, Curceanu C, Czerwiński E, Dulski K, Flak B, et al. Evaluation of single-chip, real-time tomographic data processing on FPGA SoC devices. IEEE Trans Med Imag 2018;37: 2526–35.
50. Moskal P. A hybrid TOF-PET/CT tomograph. European patent EP 3039456, 2019.
51. Moskal P. Hybrid TOF-PET/MRI tomograph. United States patent US 10,520,568, 2019.
52. Moskal P, Gajos A, Mohammed M, Chhokar J, Chug N, Curceanu C, et al. Testing CPT symmetry in ortho-positronium decays with

positronium annihilation tomography. Nat Commun 2021;12: 5658.
53. Moskal P, Dulski K, Chug N, Curceanu C, Czerwiński E, Dadgar M, et al. Positronium imaging with the novel multiphoton PET scanner. Sci Adv 2021;7:eabh4394.
54. Moskal P, Kisielewska D, Bura Z, Chhokar C, Curceanu C, Czerwiński E, et al. Performance assessment of the 2γ positronium imaging with the total-body PET scanners. EJNMMI Phys 2021;7:44.
55. Moskal P, Kisielewska D, Curceanu C, Czerwiński E, Dulski K, Gajos A, et al. Feasibility study of the positronium imaging with the J-PET tomograph. Phys Med Biol 2019;64: 055017.
56. Moskal P, Jasińska B, Stępień EŁ, Bass SD. Positronium in medicine and biology. Nature Rev Phys 2019;1:527–9.
57. Sitarz M, Cussonneau J-P, Matulewicz T, Haddad F. Radionuclide candidates for $\beta^{+}\gamma$ coincidence PET: an overview. Appl Radiat Isot 2020;155:108898.